Int J Physiol Pathophysiol Pharmacol 2021;13(3):69-85
www.ijppp.org /ISSN:1944-8171/IJPPP0133416

Original Article

Application of weighted gene co-expression network analysis to identify the hub genes in H1N1

Bo Sun[1], Xiang Guo[1], Xue Wen[2], Yun-Bo Xie[3], Wei-Hua Liu[1], Gui-Fen Pang[1], Lin-Ying Yang[1], Qing Zhang[1]

[1]Department of Respiratory and Critical Care Medicine, Affiliated Hospital of Chengde Medical University, Chengde 067000, P. R. China; [2]Department of Hematology, Affiliated Hospital of Chengde Medical University, Chengde 067000, P. R. China; [3]Department of Geriatrics, Affiliated Hospital of Chengde Medical University, Chengde 067000, P. R. China

Received March 23, 2021; Accepted June 1, 2021; Epub June 15, 2021; Published June 30, 2021

Abstract: Objective: Identifying the disease-associated interactions between different genes helps us to find novel therapeutic targets and predictive biomarkers. Methods: Gene expression data GSE82050 from H1N1 and control human samples were acquired from the NCBI GEO database. Highly co-expressed genes were grouped into modules. Through Person's correlation coefficient calculation between the module and clinical phenotype, notable modules were identified. Gene Ontology (GO) and Kyoto Encyclopedia of Genes and Genomes (KEGG) pathway analyses were conducted, and the hub genes within the module of interest were identified. Also, gene expression data GSE27131 were acquired from the GEO database to verify differential key gene expression analysis. The CIBERSORT was used to evaluate the immune cells infiltration and the GSVA was performed to identify the differentially regulated pathways in H1N1. The receiver operating characteristic (ROC) curves were used to assess the diagnostic values of the hub genes. Result: The black module was shown to have the highest correlation with the clinical phenotype, mainly functioning in the signaling pathways such as the mitochondrial inner membrane, DNA conformation change, DNA repair, and cell cycle phase transition. Through analysis of the black module, we found 5 genes that were highly correlated with the H1N1 phenotype. The H1N1 project from GSE27131 confirmed an increased expression of these genes. Conclusion: By using the WGCNA we analyzed and predicted the key genes in H1N1. BRCA1, CDC20, MAD2L1, MCM2, and UBE2C were found to be the most relevant genes, which may be therapeutic targets and predictive biomarkers for H1N1 therapy.

Keywords: H1N1, BRCA1, CDC20, MAD2L1, WGCNA

Introduction

The influenza virus infection is one of the most prevalent viral respiratory infections in the world, with more than one in five people suffering from it annually [1], containing single-stranded RNA and is classified into three types: A, B, and C [2]. The influenza A virus is a major viral influenza subtype that infects 10% of the global population annually, and poses a significant global health threat [3, 4]. Although most influenza virus infections are manageable, influenza epidemics are a large burden to the world and have substantial morbidity and mortality impacts [5, 6]. Unfortunately, the pathogenesis of influenza, which depends on both the immune system and viral determinants, is not yet fully understood. Moreover, mutation and drift allow influenza viruses to resist herd immunity and vaccination [7]. Therefore, it is critically important to investigate the pathogenesis of influenza to find effective therapeutic targets.

Weighted gene co-expression network analysis (WGCNA) is a strong clustering algorithm that can be used to detect gene co-expressions based on the microarray database and connect them to the clinical phenotype [8]. Microarray analysis is a key technique that can systematically detect the differential expression of thousands of gene expressions [9]. WGCNA can be used for detecting highly correlated genes across microarray samples based on their expressions which are clustered into different modules, these modules have different biological significance. Also, each group activation stimulates various signaling pathways that reg-

ulate multiple specific functions. WGCNA can identify the most phenotypic trait-related module while also measuring module membership [10]. Furthermore, the correlation network and modules can be implemented to identify functional enrichment and key hub genes [11]. Finding the key modules and designing the treatment targeting the key hub genes are crucial for H1N1-targeting therapies. Moreover, finding candidate biomarkers is important for prognosis, risk assessment, and monitoring disease progression.

The complex reaction mechanism of H1N1 might be uncovered through gene regulation and protein-protein interactions (PPI). An influenza A virus study in a mouse model shows that the virus could cause the differential gene expressions of 82 miRNAs and 3371 mRNAs in mice [12]. STC SWOT Analysis showed that the expressions of 46 miRNAs changed significantly during influenza A infection, and its integrated analysis of the miRNA, gene, and pathway regulatory network found that 17 miRNAs were related to the influenza A pathways. The underlying molecular mechanisms and key genes involved in H1N1 progression remain to be fully explained, suggesting a complex pathogenic mechanism of H1N1 that needs to be confirmed by further research. In this study, WGCNA was used to analyze gene expression data from H1N1-infected human samples and control human samples from a publicly available database (GEO: Gene Expression Omnibus). The team found 12 co-expression modules. Through a Pearson correlation analysis between the module and clinical phenotype, we identified one major co-expression module. Also, through the GO function and pathway enrichment analyses, we tested the biological relevance of this module and identified key hub genes with the prognosis potential. Finally, we confirmed the expression of identified key hub genes using gene expression data GSE27131. We then presented our conclusion that BRCA1, CDC20, MAD2L1, MCM2, and UBE2C are the genes most relevant to H1N1 and could be targets for novel and effective therapeutic treatments for the disease.

Materials and methods

Acquisition of gene expression data and preprocessing

This study was performed using data obtained from the NCBI's publicly available GEO database (Gene Expression Omnibus, http://www.ncbi.nlm.gov/geo). Studies were screened based on following inclusion criteria: (1) all datasets were restricted to Homo sapiens, (2) the dataset was restricted to expression profiling by array, (3) over 15 tissues were sampled in the dataset. Any study that did not meet the above criteria was excluded from selection. We chose the gene expression data GSE82050 and used the GPL21185 platform. 15 control and 20 H1N1 human samples were studied. To determine the validity of this conclusion, the identified hub genes were verified in the gene expression data GSE37131 (GPL6244 platform), which was obtained from the GEO database based on the above-described inclusion and exclusion criteria, and 7 control and 14 H1N1 human samples were analyzed. The data analysis and analytical procedures are illustrated in **Figure 1**.

The gene expression matrix was obtained and quantile normalized. We excluded some genes with low expression, and we identified 21197 significantly expressed genes. To avoid the influence of outliers, the standard deviation of the expression value was obtained. We selected the first 5000 genes, and there every probe had corresponding annotation information. Therefore, 5000 genes were considered for further study.

Structure of the weighted gene co-expression network and selection of potential biologically significant modules

R-Studio 3.6.0 software was used to cope with data and graphs. The Pearson correlation coefficient was calculated, and the gene co-expression similarity was assessed and clustered into network modules. Hierarchical clustering was used to identify modules, and we choose different colors to indicate modules. Different modules were identified using the dynamic tree cut method. Then, the adjacency matrix was transformed into a topology overlay matrix (TOM), and modules were identified by cluster analysis.

Gene modules and clinical phenotype correlation analysis

The gene expression data and clinical data were matched to detect clinically meaningful associations between modules and the clinical

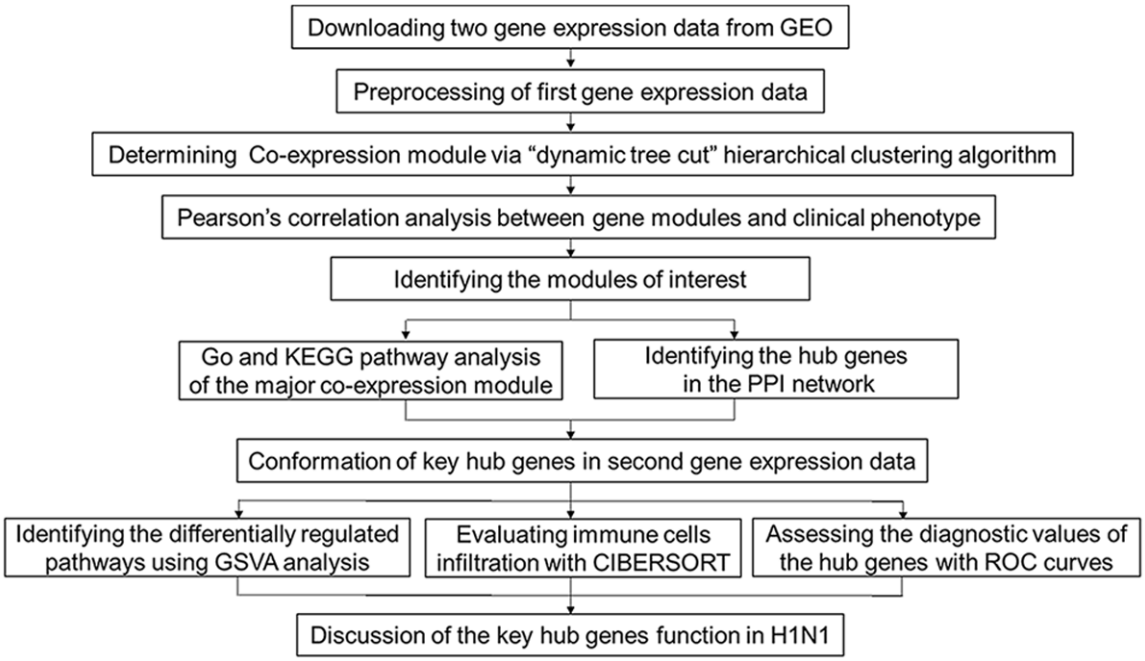

Figure 1. Flowchart of data collection procedures, data preprocessing, data analysis and discussion of this study.

phenotype. Furthermore, a Pearson correlation analysis was used to calculate the relevance between the module eigengene (ME) and the clinical phenotype. The modules with a valid relevance to the clinical phenotype were ranked and obtained. Finally, to verify the modules with valid relevance to clinical phenotype, the relationship between Module Membership (MM) and Gene Significance (GS) was evaluated and the *p*-values were calculated.

GO terms and KEGG pathway analyses, identification, and confirmations of hub genes, PPI analysis, and other analyses

GO and KEGG pathways enrichment analyses were performed. To better understand the pathogenesis, reconstruction of pathways were arranged additionally. GO enrichment analysis and KEGG pathways enrichment analyses were carried out using the R package clusterProfiler to comprehensively explore the functions of the black module [13]. GO terms and KEGG pathways with a *p*-value less than 0.05 were considered to be significantly enriched. Subsequently, we used the cytoHubba application in Cytoscapecto to select the key hub genes. Next, by the usage of GeneMANIA, we constructed the network through PPI analysis to confirm the identified hub genes. In addition, to further confirm the selected hub genes, GSE27131 was used to verify differential key gene expression analysis. Furthermore, we used CIBERSORT to evaluate the immune cells infiltration and the GSVA was performed to identify the differentially regulated pathways in H1N1. Finally, the ROC curves were used to assess the diagnostic values of the hub genes.

Results

Sample selection and data preprocessing

Gene expression data GSE82050 contains 21197 genes. The 35 groups of subjects were then analyzed by RStudio 3.6.0 software.

Weighted gene co-expression network structure and disease module recognition

WGCNA was used to construct gene co-expression networks that correlated with the H1N1 phenotype. We performed the scale independence and mean connectivity analysis, and our results showed that when the soft threshold power value equaled 7, scale independence was larger than 0.85, and mean connectivity was approximated to zero, so the weighted value was set to 7 (**Figure 2**). We classified the genes according to the expression pattern

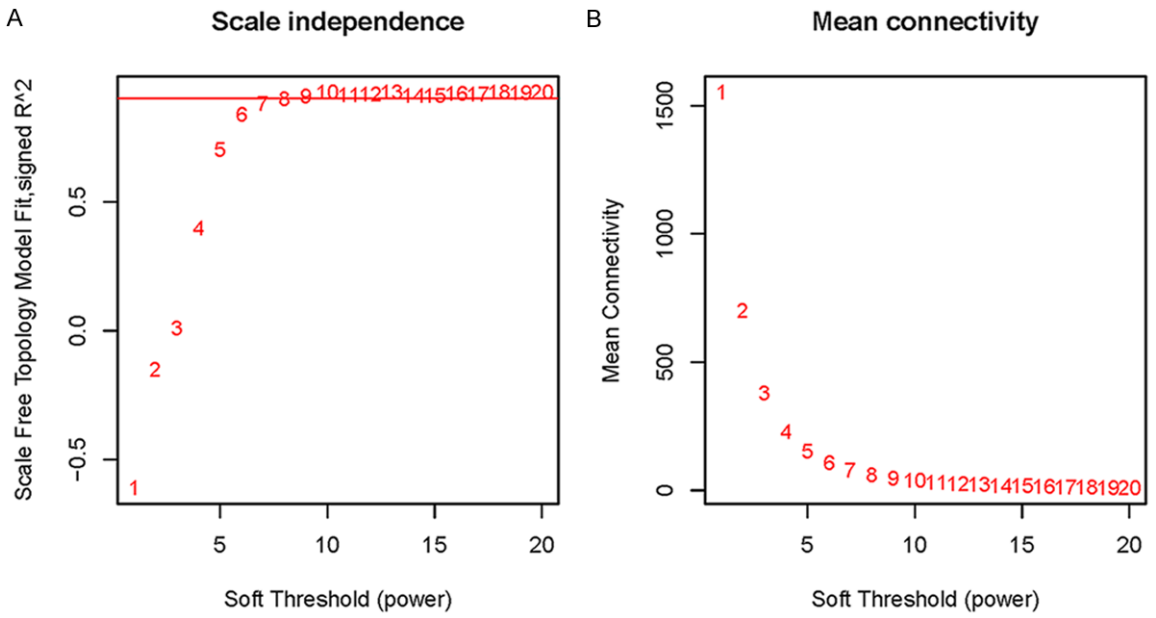

Figure 2. Analysis of soft-thresholding power in weighted gene co-expression network analysis. The red line represents a scale independence of 0.85 (A) and mean connectivity was approximate to zero (B) when the soft threshold power value equals 7.

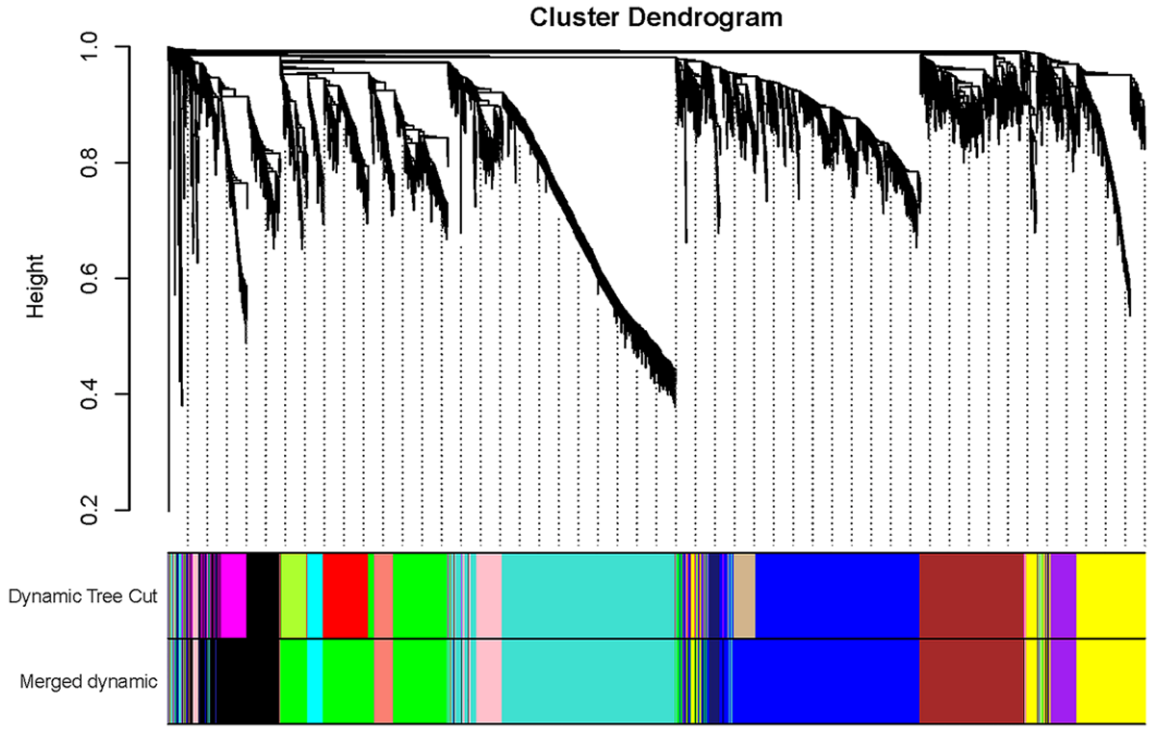

Figure 3. WGCNA of gene expression in H1N1 identifies modules of correlated genes.

derived from the correlation coefficient calculation, then grouped patterned genes into one module. We identified twelve modules in the range of 11 to 1116 genes, and every module was assigned a unique color (**Figure 3**; **Table 1**).

Identification of module of interest and correlation analysis

Results showed the black module and clinical phenotype have the strongest association

Table 1. Module and the corresponding gene count

Module	Gene count	Module	Gene count	Module	Gene count
Black	449	Blue	1116	Brown	541
Cyan	85	Green	753	Grey	11
Midnight blue	61	Pink	206	Purple	145
Salmon	127	Turquoise	1053	Yellow	453

(r=0.64, P=3e-05). Therefore, the black module was selected as the critical module in follow-up analyses. To validate the correlation, we calculated the associated module membership values with gene significance (MMSE) via the Heatmap function. The Heatmap function showed strong relevance between module membership with gene significance in MMSE (correlation coefficient =0.46, P=6.8e-25) in the black module (**Figure 4**). Next, GO functional and KEGG pathway analyses were performed to explore the biological functions and biological pathways of genes in the black module. In the KEGG pathway analysis, the mitochondrial inner membrane, DNA conformation change, DNA repair, cell cycle phase transition, and condensed chromosome signaling pathway were found to be the most valid pathways in the black module (**Figure 5**).

The identified black module was further analyzed via GO enrichment analysis and KEGG enrichment analyses using the R package clusterProfiler. As shown in **Figure 6**, a high number of genes were significantly enriched in chromosome segregation, mitotic nuclear division, and electron transport chain in the category biological process; mitochondrial inner membrane, mitochondrial protein complex, and chromosomal region in the category cellular component; and structural constituent of ribosome and electron transfer activity in the molecular function category (**Figure 6A**). Furthermore, the KEGG pathway analysis (**Figure 6B**) revealed that the most significantly enriched pathways of the genes were related to pathways of neurodegeneration and oxidative phosphorylation (P<0.005).

Identification and confirmations of key hub genes, PPI analysis, and other analyses

There were 449 genes polymerized in the black module. Subsequently, we used Cytoscape to visualize the hub genes in the black module (**Figure 7**). A total of 5 genes were identified as key hub genes, and they were validated and studied with the use of GeneMANIA. A PPI network was constructed to analyze the genes interconnected with BRCA1, CDC20, MAD2L1, MCM2, and UBE2C (**Figure 8**). The network of genes in the black module involved 25 hub genes, containing the top 5 hub genes. Furthermore, in the GSE27131, 24502 genes were identified; the platform was GPL6244. The gene expression of 7 control samples and 14 H1N1 samples were analyzed to verify the differential expression of the 5 hub genes that we had ascertained at the previous step. The results showed that there were significant differences in the expression of these 5 hub genes between the control and H1N1 human samples (P<0.05) (**Figure 9**). All of these findings further confirmed our identification of these 5 hub genes.

In addition, the CIBERSORT was used to evaluate the infiltration of the immune cells. A strong correlation between 5 top hub genes and immune cell content was noted (**Figure 10**). Moreover, GSVA was performed to identify the differentially regulated pathways in H1N1. Results showed that all 5 hub genes were involved in the E2F-TARGETS pathway, and three of the hub genes (BRCA1, MCM2, UBE2C) were involved in the XENOBIOTIC-METABOLISM (**Figure 11**).

Finally, the ROC curves were used to assess the diagnostic values of the hub genes (**Figure 12**). The time-dependent ROC analysis has the best capacity to predict diagnostic efficiency compared with that of other properties. And the protein-protein interaction plot was constructed for correlation analysis of 5 hub genes (**Figure 13**).

Discussion

Influenza A viruses (IAVs) remain a substantial threat to global health, causing millions of cases of moderate to severe illness [14]. The pathogenesis of H1N1 is complex and unclear, and therefore, clinical prevention and treatment are difficult to administer. Studies show that the influenza A viral infection leads to cell necrocytosis and apoptosis [15, 16], immune

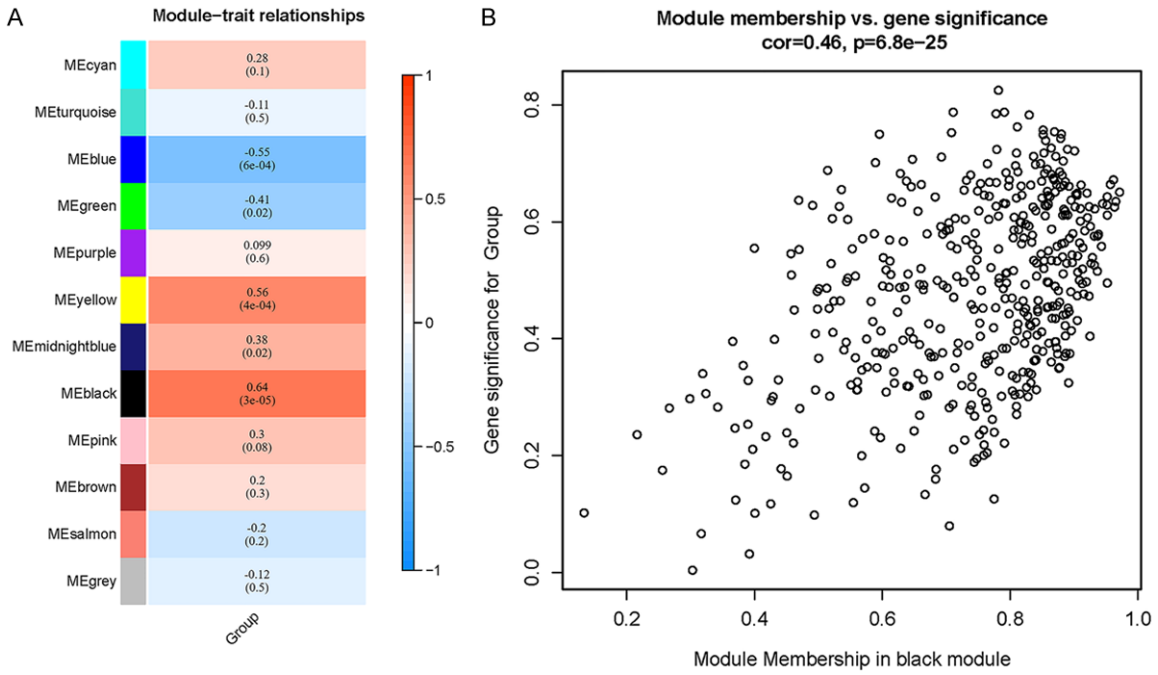

Figure 4. Objective modules analysis. A. Module-trait relationships. B. Correlation between module membership and gene significance of genes in black module.

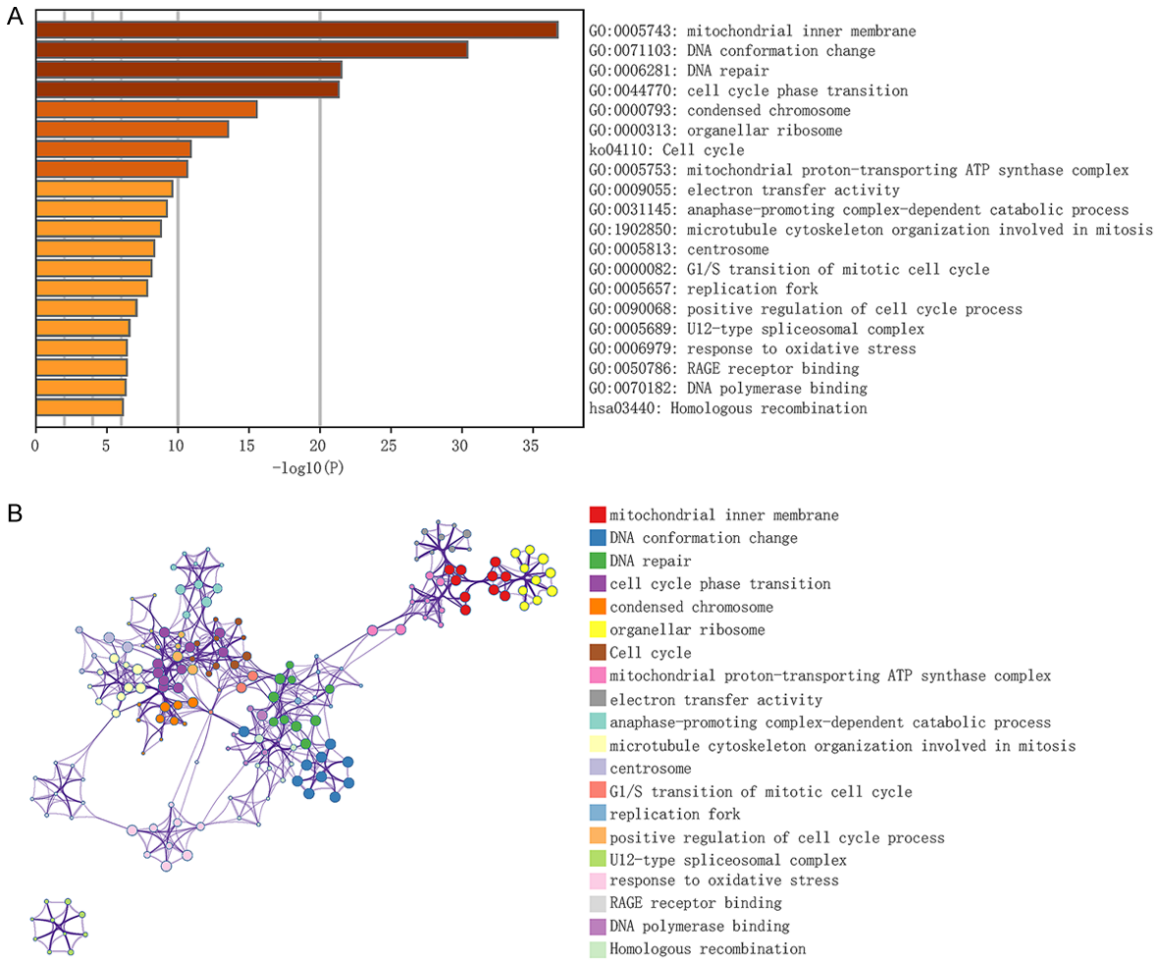

Figure 5. A. GO enrichment and KEGG pathway analyses. B. Interaction network of pathways. The nodes represent the pathways.

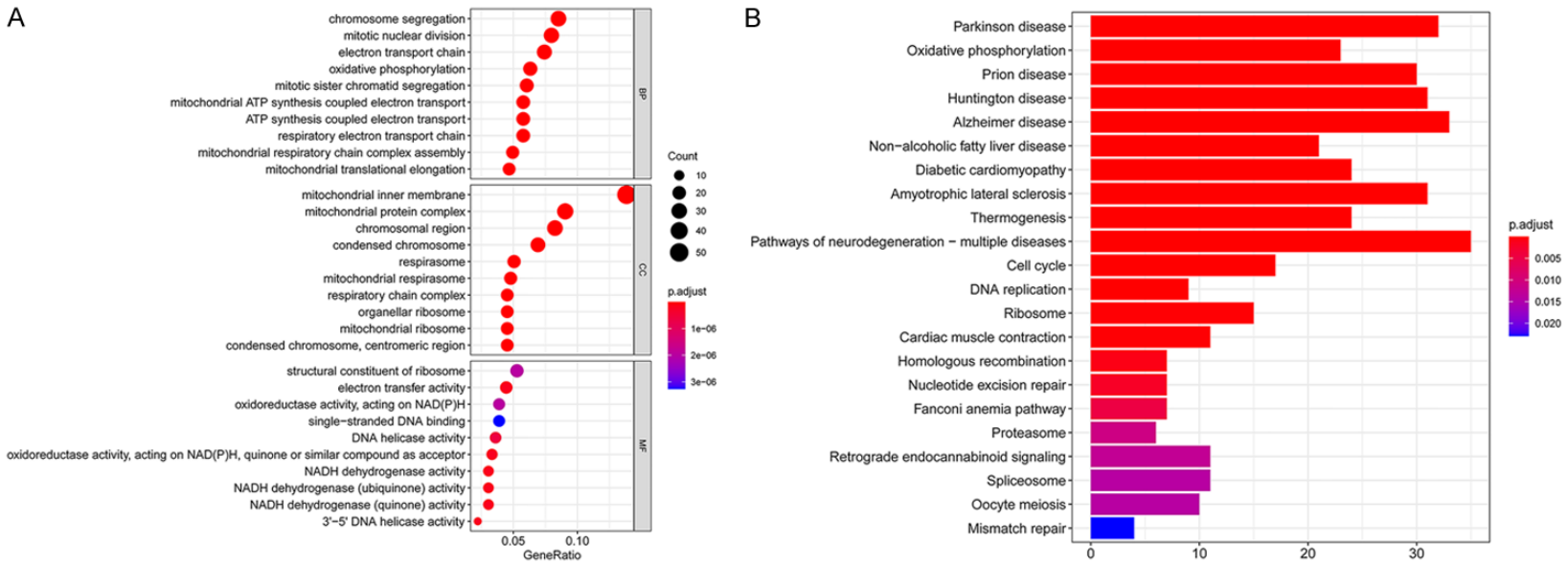

Figure 6. Functional enrichment analysis of the black module. GO enrichment analysis of genes in black module. A. GO analysis divided genes in the black module into three functional groups: biological process (BP), cellular component (CC), and molecular function (MF). B. KEGG pathway enrichment analysis of the genes in black module. The size of the dots represented the number of enriched genes. From purple to red, the *P* value decreased.

Identifying the hub genes in H1N1 by WGCNA

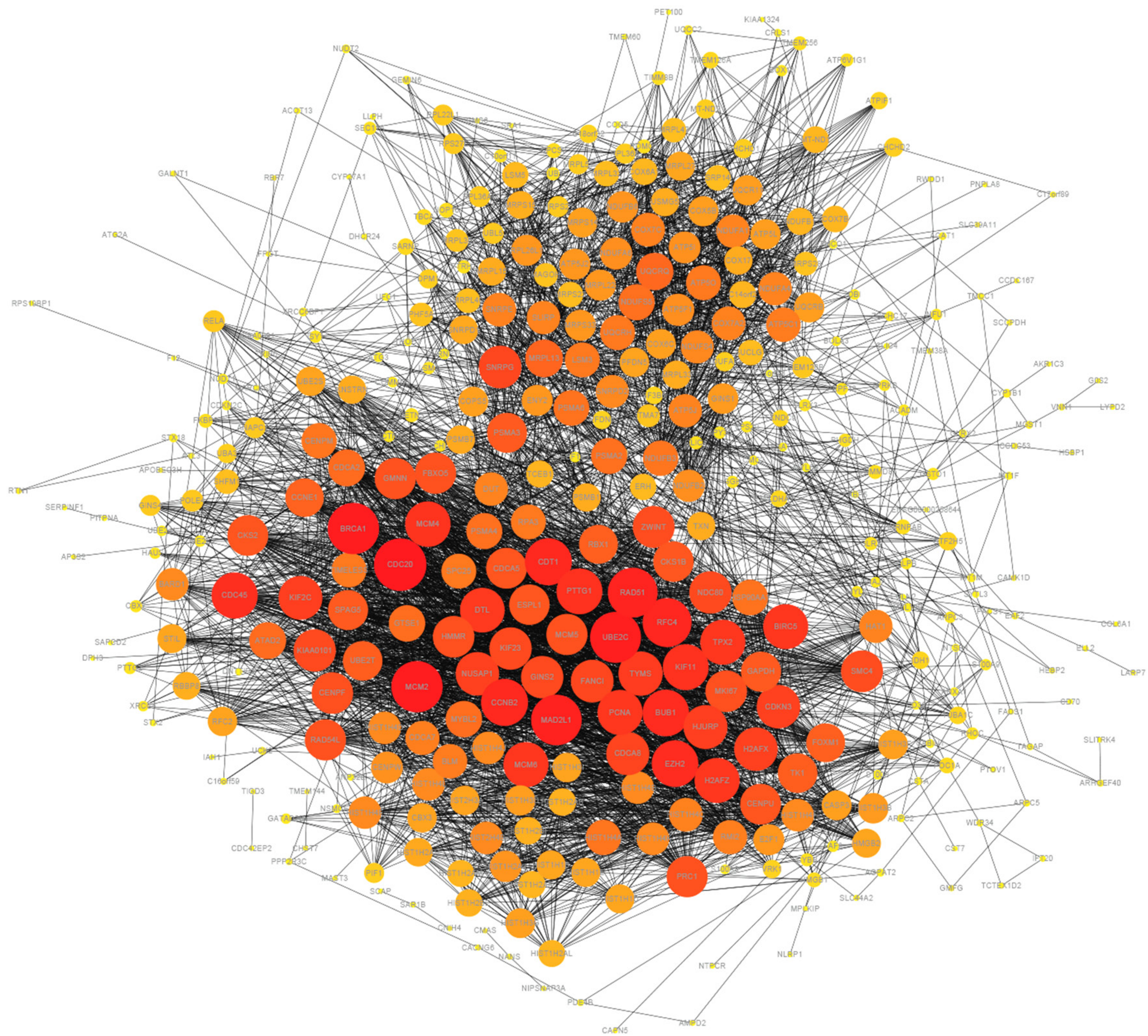

Figure 7. Visualization of the correlation network from the black module: Cytoscape analysis identified 5 genes (BRCA1, CDC20, MAD2L1, MCM2, and UBE2C) are hub nodes in the network.

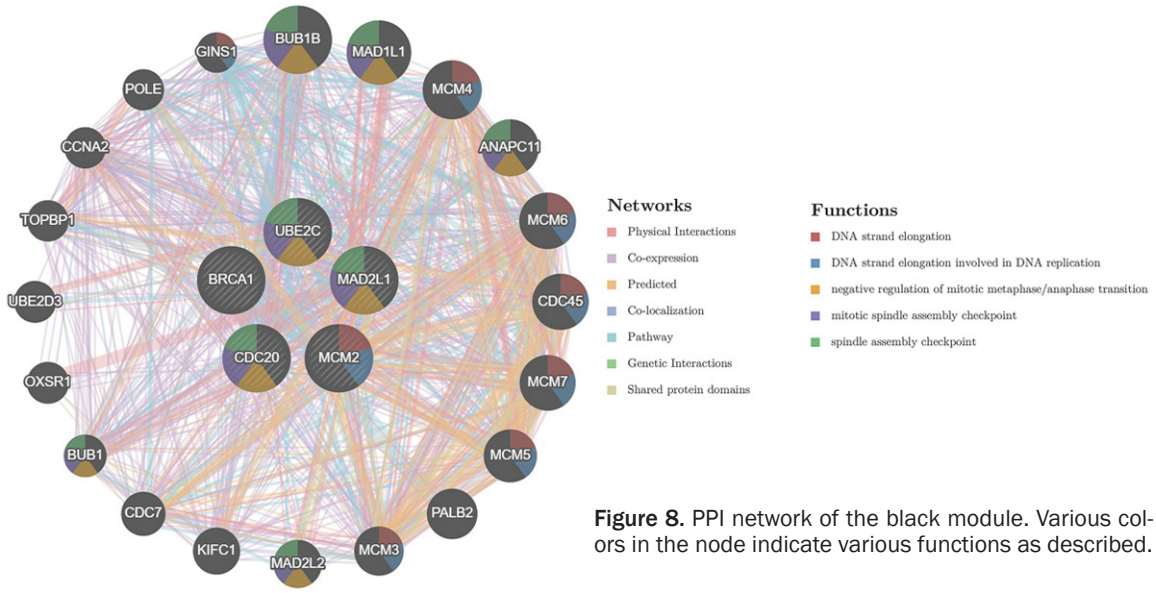

Figure 8. PPI network of the black module. Various colors in the node indicate various functions as described.

dysfunction [17], and coagulation dysfunction [18]. Although a number of previous studies have investigated pathogenesis of H1N1, to the best of our knowledge, H1N1 has been seldom studied using bioinformatic analysis method. Among the 5 key genes we have identified in this study, CDC20 and MAD2L1 have never been mentioned in the study of the mechanism of human influenza. This is the novelty of the present study, and it deserves emphasis.

First, we used the WGCNA to analyze the entire genome expression data and choose GSE82050 for the analysis of gene expression in this database. Then, we identified 35 co-expressed modules to assess the biological information that is relevant to H1N1. Each co-expressed module contained highly correlated genes. Through Pearson's correlation coefficient calculation, we found one module (the black module) significantly related to H1N1. Furthermore, GO and KEGG pathway analyses showed that the mitochondrial inner membrane, DNA conformation change, DNA repair, cell cycle phase transition, and condensed chromosome signaling pathway were the most important pathways in the black module. Furthermore, we identified the hub genes with a strong correlation in the black module. With further verification in the second database GSE27131, which was obtained from GEO, BRCA1, CDC20, MAD2L1, MCM2, and UBE2C were identified to be the key hub genes in correlation with H1N1.

The analysis showed that BRCA1 plays a considerable role in H1N1 etiopathogenesis. BRCA1 was first found in human breast cancer cells. Further studies have found that BRCA1 is involved in DNA damage repair, cell cycle control, and regulation of gene transcription [19]. In addition, BRCA1 can be a tumor-inhibiting factor; it has been shown to inhibit the nuclease activity in vitro [20]. Therefore, BRCA1 is a potential target in the prevention and treatment of some tumors. The latest research shows that in breast cancer [21], ovarian cancer [22], and liver cancer [23], the BRCA1 mutation is closely related to the infiltrating degree of immune cells, and it could be a new indicator to assess the condition of these diseases. In our study, the H1N1 group and healthy control group were compared in terms of their BRCA1 expression levels. The BRCA1 expression level was much higher in the H1N1 group compared to the healthy control group, and it was associated with high infiltration of immune cells (para-inflammation-expressing cells, B_cells, and human leukocyte antigen). These results suggest that BRCA1 may be a key gene in the

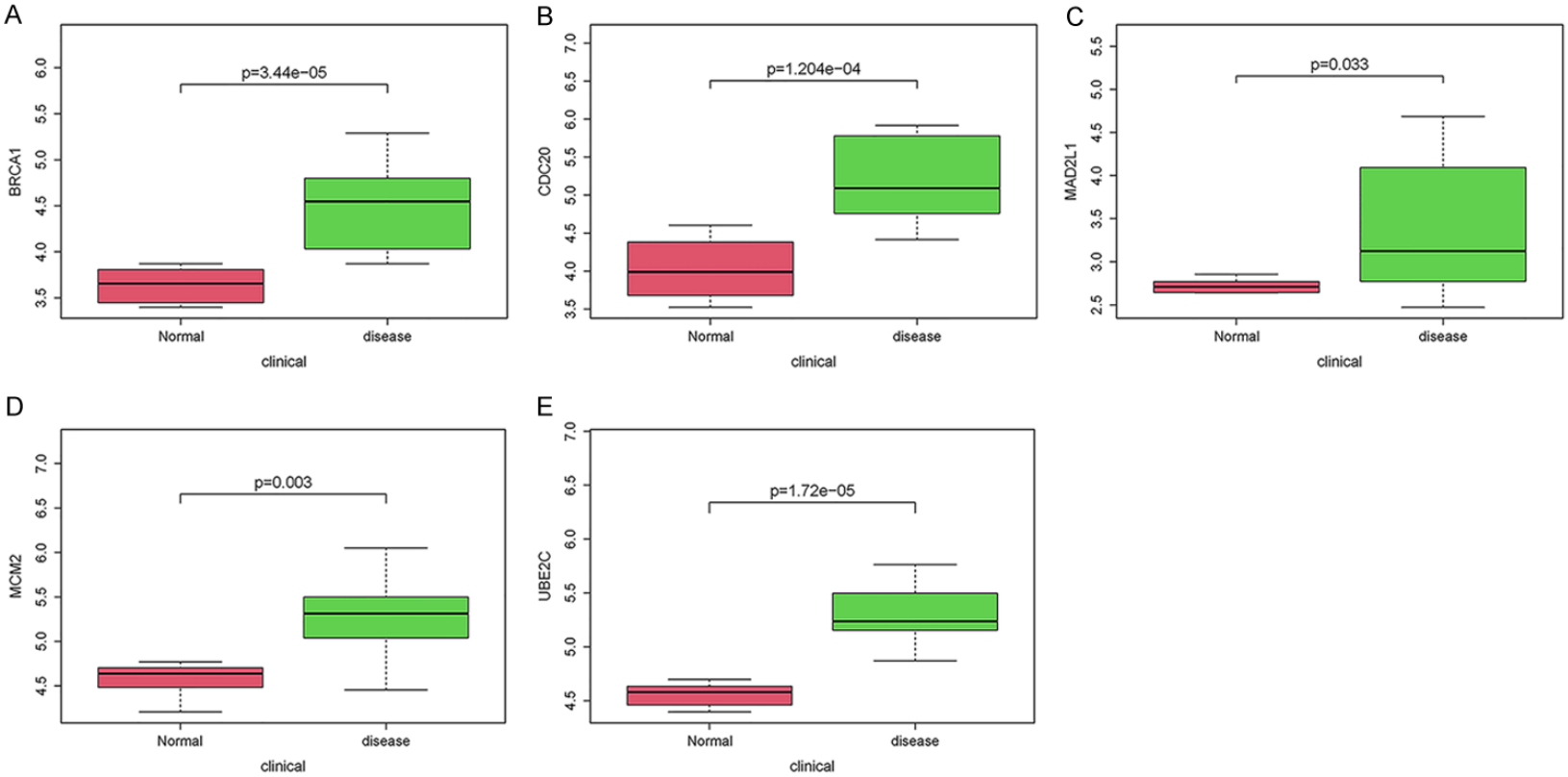

Figure 9. The differential expression of 5 top hub genes between the control and H1N1 human samples (P<0.05) in the GSE27131.

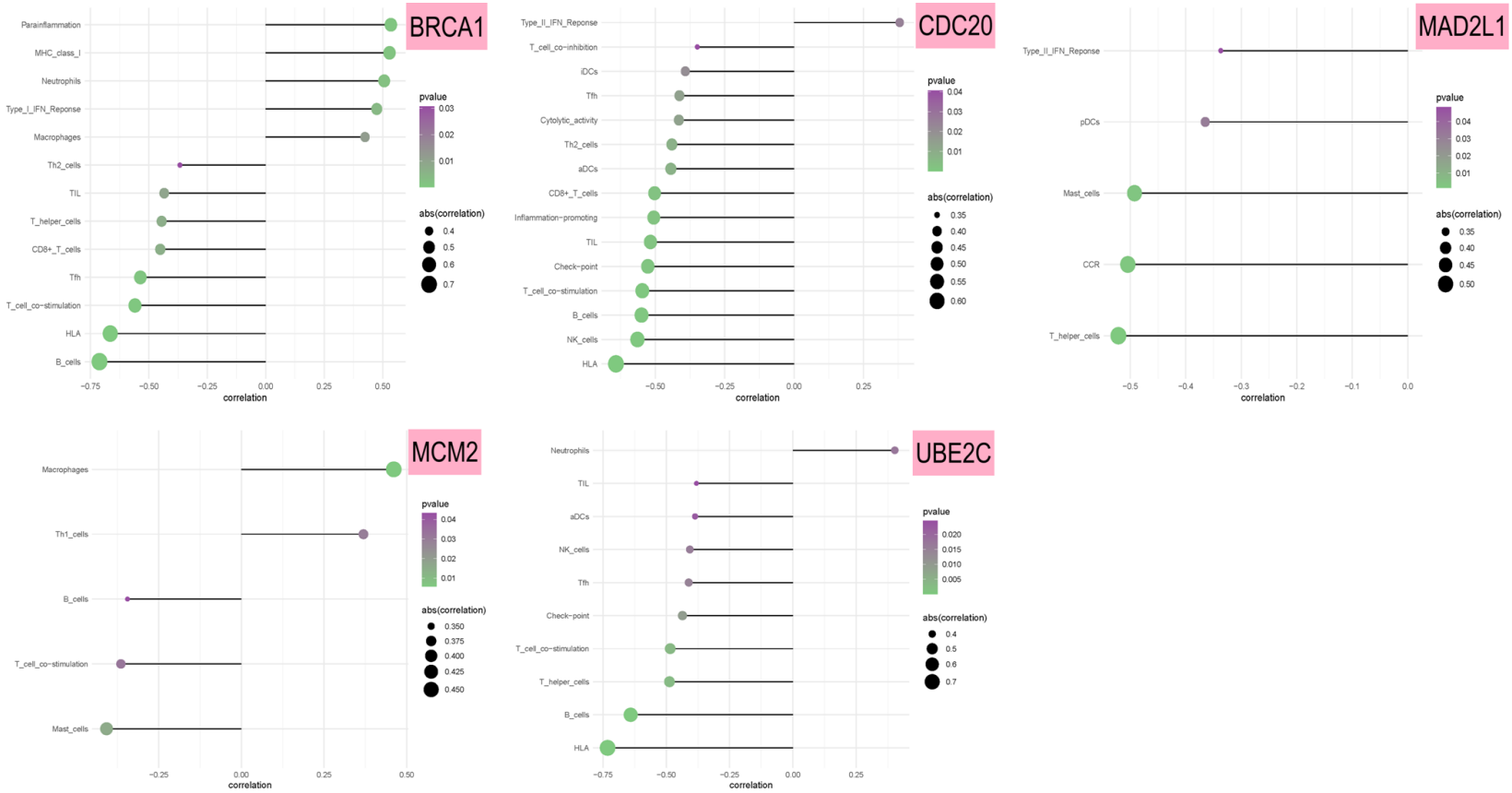

Figure 10. Correlation between 5 hub genes and immune cell content.

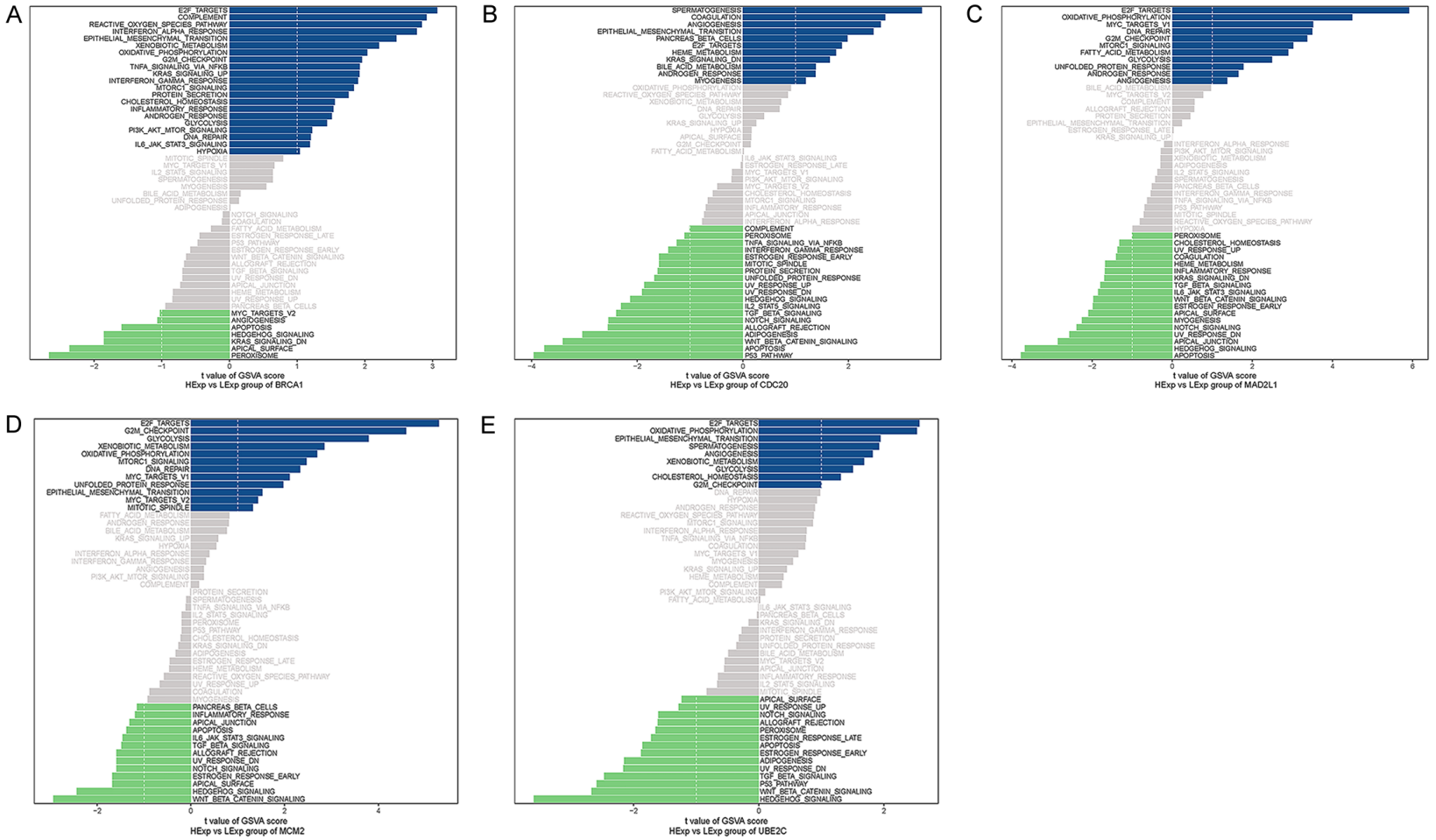

Figure 11. GSVA was performed to identify the differentially regulated signaling pathways in H1N1. HExp stands for high expression and LExp stands for low expression.

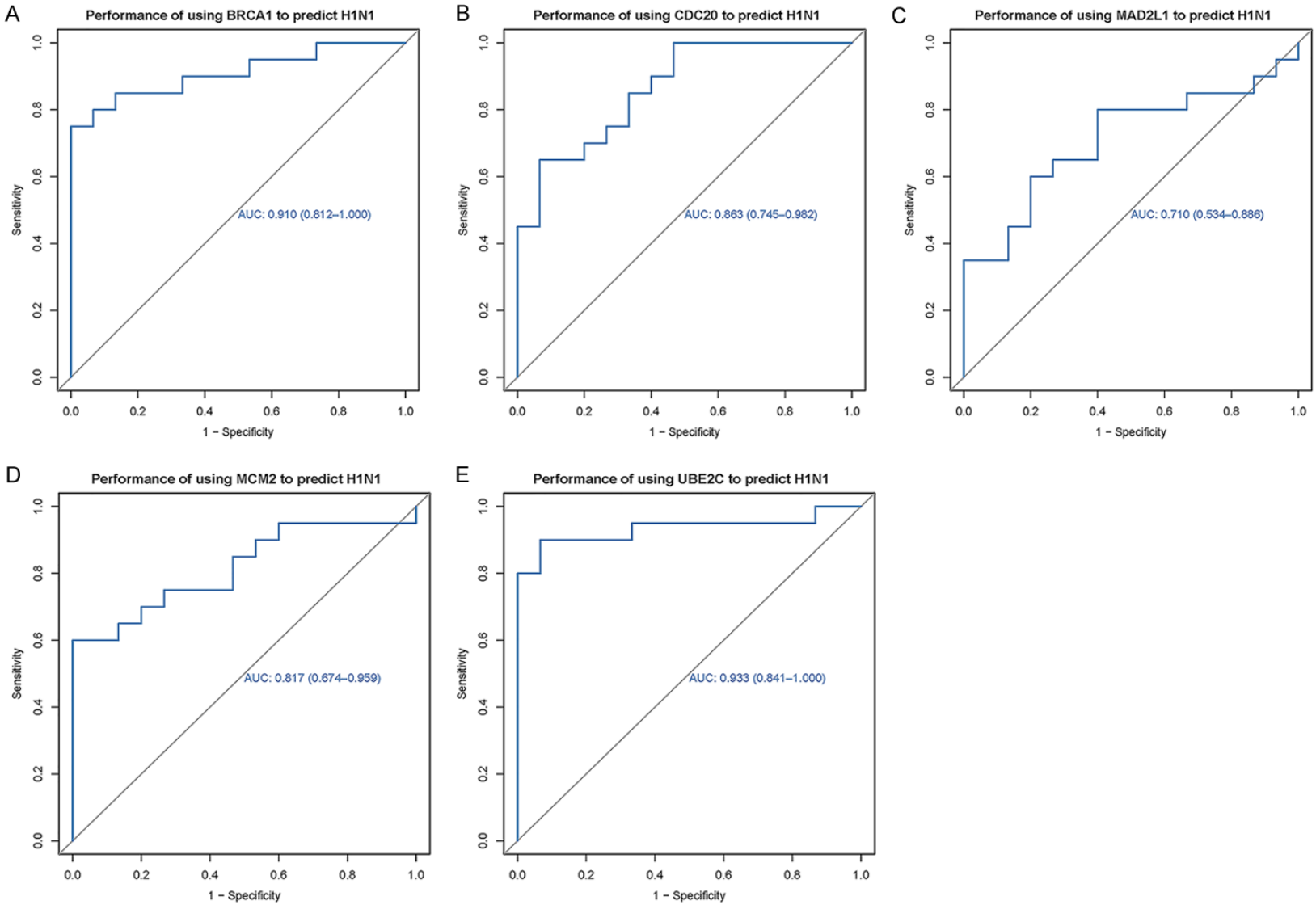

Figure 12. ROC curves of the 5 hub genes. ROC curves were used to assess the diagnostic values and predictive values of 5 hub genes.

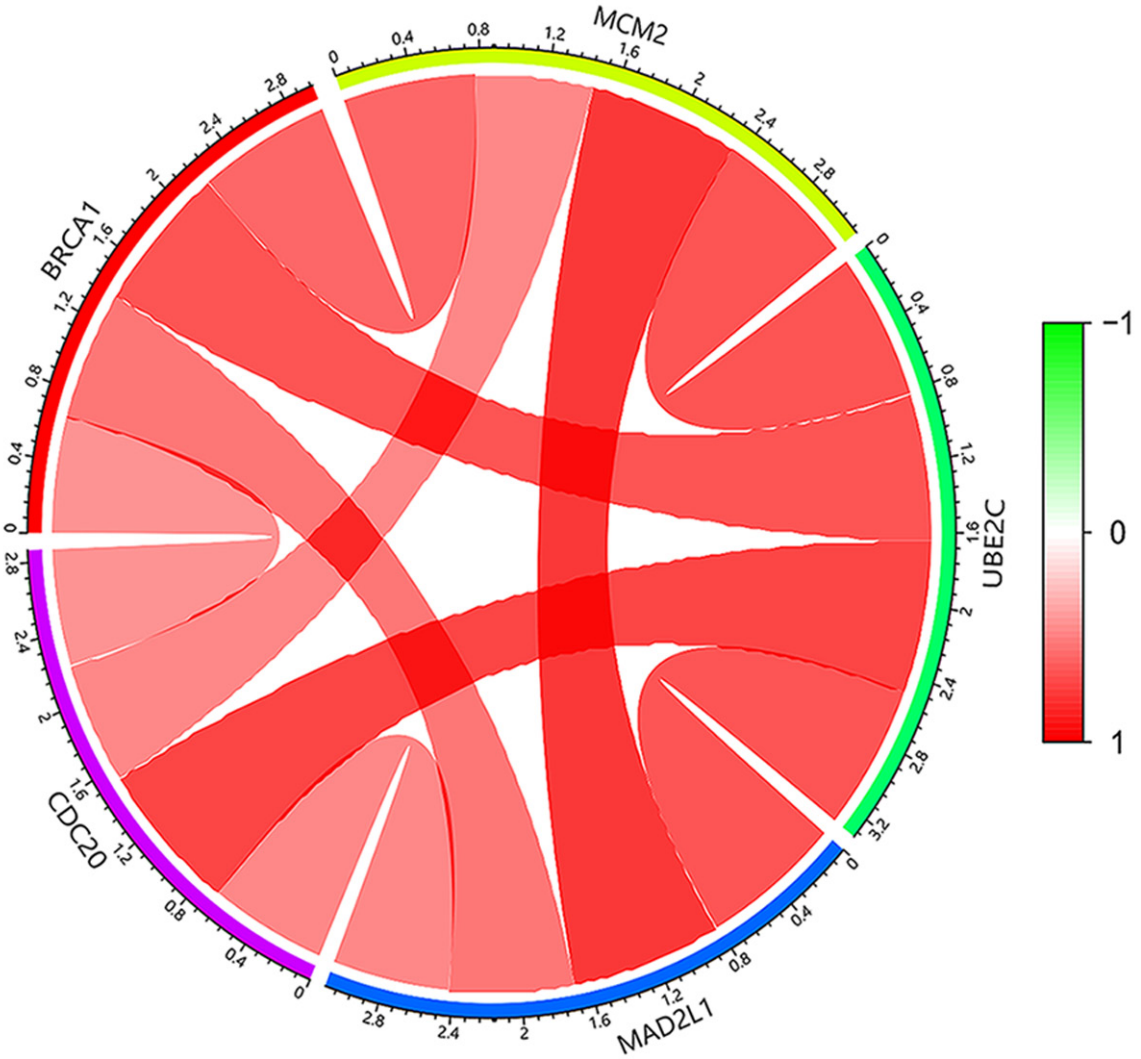

Figure 13. Correlation analysis of the 5 hub genes. Protein-protein interaction of 5 hub genes of HIN1.

inflammatory response induced by the influenza A virus. Targeting BCRA1 may be a novel therapeutic strategy.

CDC20 was detected as another important factor of the H1N1 in this study. CDC20 (Cell Division Cycle 20) plays a vital role in cell cycle and chromosome dynamics during mitosis [24]. In addition, it is also involved in the regulation of apoptosis, brain development, and the occurrence and development of tumors. In a study of lung adenocarcinoma by WGCNA [19], 15 co-expressed SRGs (CDC20, CDCA5, CDCA8, CCNA2, CCNB1, FEN1, KPNA2, RRM2, SPAG5, TOP2, MCM6, KIF2C, NUSAP1, RACGAP1, and TPX2) were identified, and the overexpression of SRGs, such as CDC20, was associated with reduced immune infiltration. Meanwhile, overexpression of CDC20 predicts a poor prognosis in different types of lung cancer [25, 26]. In our study, influenza A virus-induced overexpression of CDC20 contributes to excessive infiltration of immune cells. Previous studies have shown that the high expression of CDC20 is related to the occurrence and development of tumors. However, it has not yet been reported whether CDC20 is involved in the inflammatory response. Our study revealed that CDC20 also has a pro-inflammatory effect.

In the network analysis, the MAD2L1 (Mitotic arrest deficient 2-like protein 1) gene was identified as another key hub gene. Previous data shows that MAD2L1 is essential for the survival

of cancer cell lines. For example, the vast majority of cancer cell lines highly express MAD2L1, thereby suggesting that MAD2L1 was significantly associated with higher clinical stage and histological grade of breast cancer [27]. While in lung adenocarcinoma tissue, MAD2L1 gene expression may predict poor overall survival in patients and increase the risk of recurrence, and it may function as a prognostic biomarker of lung adenocarcinoma [28]. In addition, it was found that the expression of MAD2L1 significantly correlated with several tumor indicators, including HER-2, Ki-67, ER, and P53 [27]. The overexpression of MAD2L1 can change the structure of chromosomes and further lead to abnormal cell proliferation and cell differentiation. In this study, it was found that the overexpression of MAD2L1 was closely related to the various pathological changes of H1N1, and it correlated with the degree of macrophage infiltration.

The minichromosome maintenance family (MCMs) is a group of proteins involved in DNA synthesis. Among them, the MCM2-7 protein complex functions as an essential replicative helicase for DNA replication [29]. Studies have shown that the abnormalities of MCMs contribute to tumorigenesis through regulating the cell cycle and DNA damage [30]. Overexpression of MCMs has been found in different human cancer cells [31]. However, no previous studies have evaluated the potential effect of MCM in inflammation, and our study indicates that MCM has a pro-inflammatory effect.

At last, the ubiquitin-conjugating enzyme 2C (UBE2C) was identified as another hub gene, and it has been shown that genome instability can be enhanced by the overexpression of UBE2C, which can lead to several different cancers [32]. In our study, UBE2C is highly expressed in the H1N1 group and accompanied by immune cell infiltration, therefore, UBE2C may be a potential indicator of H1N1-induced inflammation.

BRCA1, CDC20, MAD2L1, MCM2, and UBE2C are the key factors in cell cycle regulation. A growing number of studies have shown that overexpression of these key factors is associated with tumorigenesis and malignancies. In this study, we found that the overexpression of these key factors was significantly elevated in H1N1 patients. Inflammation is a biological response of the immune system that can be triggered by the influenza A virus. Inflammatory cells can be activated by inflammation, leading to the induction and activation of several oxidant-generating enzymes, which can produce different oxidants and free radicals. The reaction of different free radicals and oxidants leads to the generation of other more potent reactive oxygen and nitrogen species, causes the damage of RNA, DNA, proteins, and lipids by different reactions, increases mutations, and contributes to carcinogenesis [33]. The study indicated that suitable inflammation therapy should be investigated for the prevention of cancers. Also, these genes appeared to be strongly associated with immune cell infiltration, and the results showed that the identified 5 key genes significantly correlated with the E2F_TARGETS pathway, suggesting that these key genes play a critical role as a key regulator of the cell cycle. Through an analogical method, Zarei Ghobadi M, et al. have found 38 modules correlated to influenza infection and showed a sequence of key factors in pediatric influenza using microarray data from the pediatric influenza-infected samples [33]. In the screening of key genes, we found many key genes in common, such as the UBE2 gene. Consistently, innate immune response and cell cycle events were observed to be functional categories that were enriched in pediatric influenza. Our findings echo with reports in this literature.

In conclusion, through WGCNA, we discovered BRCA1, CDC20, MAD2L1, MCM2, and UBE2C as key hub genes in H1N1. Greater exploration of the ascertained hub genes is needed to comprehend the H1N1 mechanisms. These candidate genes and related proteins could be used as biomarkers and for drug targeting. However, further research is required to confirm these observations.

Disclosure of conflict of interest

None.

Address correspondence to: Qing Zhang, Department of Respiratory and Critical Care Medicine, Affiliated Hospital of Chengde, No. 36, Nanyingzi Street, Shuangqiao District, Chengde 067000, P. R. China. Tel: +86-15633142668; E-mail: zhangqing0668@163.com

References

[1] Tang BM, Shojaei M, Teoh S, Meyers A and Schughart K. Neutrophils-related host factors associated with severe disease and fatality in patients with influenza infection. Nat Commun 2019; 10: 3422.

[2] Stefan R, Delphine G and Stephen C. An in vitro fluorescence based study of initiation of RNA synthesis by influenza B polymerase. Nucleic Acids Res 2017; 45: 3353-3368.

[3] Liu Y, Tan HX, Koutsakos M, Jegaskanda S, Esterbauer R, Tilmanis D, Aban M, Kedzierska K, Hurt AC and Kent SJ. Cross-lineage protection by human antibodies binding the influenza B hemagglutinin. Nat Commun 2019; 10: 324.

[4] Aegerter H, Kulikauskaite J, Crotta S, Patel H, Kelly G, Hessel EM, Mack M, Beinke S and Wack A. Influenza-induced monocyte-derived alveolar macrophages confer prolonged antibacterial protection. Nat Immunol 2020; 21: 145-157.

[5] Liu X, Zhang B, Wang Y, Haymour HS and Low PS. A universal dual mechanism immunotherapy for the treatment of influenza virus infections. Nat Commun 2020; 11: 5597.

[6] Toots M, Yoon JJ, Cox RM, Hart M and Plemper RK. Characterization of orally efficacious influenza drug with high resistance barrier in ferrets and human airway epithelia. Sci Transl Med 2019; 11: eaax5866.

[7] Deng L, Mohan T, Chang TZ, Gonzalez GX, Wang Y, Kwon YM, Kang SM, Compans RW, Champion JA and Wang BZ. Double-layered protein nanoparticles induce broad protection against divergent influenza A viruses. Nat Commun 2018; 9: 359.

[8] Yang R, Du Y, Wang L, Chen Z and Liu X. Weighted gene co-expression network analysis identifies CCNA2 as a treatment target of prostate cancer through inhibiting cell cycle. J Cancer 2020; 11: 1203-1211.

[9] C. CA, Thomas S, Razvan S, Picard KC, Picard SC, Lu TH, Franklin KR, French SJ, Gerald P and Mick C. GeneSigDB-a curated database of gene expression signatures. Nucleic Acids Res 2010; 38: D716-D725.

[10] Qin J, Yang T, Zeng N, Wan C and Wen F. Differential coexpression networks in bronchiolitis and emphysema phenotypes reveal heterogeneous mechanisms of chronic obstructive pulmonary disease. J Cell Mol Med 2019; 23: 6989-6999.

[11] van Dam S, Võsa U, van der Graaf A, Franke L and de Magalhães JP. Gene co-expression analysis for functional classification and gene-disease predictions. Brief Bioinform 2018; 19: 575-592.

[12] Bao Y, Gao Y, Jin Y, Cong W, Pan X and Cui X. MicroRNA expression profiles and networks in mouse lung infected with H1N1 influenza virus. Mol Genet Genomics 2015; 290: 1885-1897.

[13] Yu G, Wang LG, Han Y and He QY. ClusterProfiler: an R package for comparing biological themes among gene clusters. Omics 2012; 16: 284-287.

[14] Van Kerkhove MD, Vandemaele KA, Shinde V, Jaramillo-Gutierrez G, Koukounari A, Donnelly CA, Carlino LO, Owen R, Paterson B, Pelletier L, Vachon J, Gonzalez C, Hongjie Y, Zijian F, Chuang SK, Au A, Buda S, Krause G, Haas W, Bonmarin I, Taniguichi K, Nakajima K, Shobayashi T, Takayama Y, Sunagawa T, Heraud JM, Orelle A, Palacios E, van der Sande MA, Wielders CC, Hunt D, Cutter J, Lee VJ, Thomas J, Santa-Olalla P, Sierra-Moros MJ, Hanshaoworakul W, Ungchusak K, Pebody R, Jain S and Mounts AW; WHO Working Group for Risk Factors for Severe H1N1pdm Infection. Risk factors for severe outcomes following 2009 influenza A (H1N1) infection: a global pooled analysis. PLoS Med 2011; 8: e1001053.

[15] Kumova OK, Fike AJ, Thayer JL, Nguyen LT and Carey AJ. Lung transcriptional unresponsiveness and loss of early influenza virus control in infected neonates is prevented by intranasal Lactobacillus rhamnosus GG. PLoS Pathog 2019; 15: e1008072.

[16] Atkin-Smith GK, Duan M, Chen W and Poon IKH. The induction and consequences of Influenza A virus-induced cell death. Cell Death Dis 2018; 9: 1002.

[17] Darwish I, Mubareka S and Liles WC. Immunomodulatory therapy for severe influenza. Expert Rev Anti Infect Ther 2011; 9: 807-822.

[18] Schouten M, Sluijs KF, Gerlitz B, Grinnell BW, Roelofs JJ, Levi MM, van 't Veer C and van der Poll T. Activated protein C ameliorates coagulopathy but does not influence outcome in lethal H1N1 influenza: a controlled laboratory study. Crit Care 2010; 14: R65.

[19] Paterson JW. BRCA1: a review of structure and putative functions. Dis Markers 2014; 13: 261-274.

[20] Jhanwar UM. BRCA1 in cancer, cell cycle and genomic stability. Front Biosci 2003; 8: s1107-1117.

[21] Sønderstrup IMH, Jensen MB, Ejlertsen B, Eriksen JO, Gerdes AM, Kruse TA, Larsen MJ, Thomassen M and Laenkholm AV. Evaluation of tumor-infiltrating lymphocytes and association with prognosis in BRCA -mutated breast cancer. Acta Oncol 2019; 58: 363-370.

[22] Clarke B, Tinker AV, Lee CH, Subramanian S, Matt VDR, Turbin D, Kalloger S, Han G, Ceballos K and Cadungog MG. Intraepithelial T cells and prognosis in ovarian carcinoma: novel associations with stage, tumor type, and BRCA1 loss. Mod Pathol 2009; 22: 393-402.

[23] Mei J, Wang R, Xia D, Yang X and Liu C. BRCA1 is a novel prognostic indicator and associates with immune cell infiltration in hepatocellular carcinoma. DNA Cell Biol 2020; 39: 1838-1849.
[24] Zhang MY, Liu XX, Li H, Li R, Liu X and Qu YQ. Elevated mRNA Levels of AURKA, CDC20 and TPX2 are associated with poor prognosis of smoking related lung adenocarcinoma using bioinformatics analysis. Int J Med Sci 2018; 15: 1676-1685.
[25] Kato T, Daigo Y, Aragaki M, Ishikawa K, Sato M and Kaji M. Overexpression of CDC20 predicts poor prognosis in primary non-small cell lung cancer patients. J Surg Oncol 2012; 106: 423-430.
[26] Dong S, Huang F, Zhang H and Chen Q. Overexpression of BUB1B, CCNA2, CDC20 and CDK1 in tumor tissues predicts poor survival in pancreatic ductal adenocarcinoma. Biosci Rep 2019; 39: BSR20182306.
[27] Zhu XF, Yi M, He J, Tang W, Lu MY, Li T and Feng ZB. Pathological significance of MAD2L1 in breast cancer: an immunohistochemical study and meta analysis. Int J Clin Exp Pathol 2017; 10: 9190-9201.
[28] Shi YX, Zhu T, Zou T, Zhuo W and Liu ZQ. Prognostic and predictive values of CDK1 and MAD2L1 in lung adenocarcinoma. Oncotarget 2016; 7: 85235-85243.
[29] Das SP and Rhind N. How and why multiple MCMs are loaded at origins of DNA replication. Bioessays 2016; 38: 613-617.
[30] Wang Y, Chen H, Zhang J, Cheng ASL, Yu J, To KF and Kang W. MCM family in gastrointestinal cancer and other malignancies: from functional characterization to clinical implication. Biochim Biophys Acta Rev Cancer 2020; 1874: 188415.
[31] Yu S, Wang G, Shi Y, Xu H and Chen Y. MCMs in cancer: prognostic potential and mechanisms. Anal Cell Pathol (Amst) 2020; 2020: 3750294.
[32] Xie C, Powell C, Yao M, Wu J and Dong Q. Ubiquitin-conjugating enzyme E2C: a potential cancer biomarker. Int J Biochem Cell Biol 2014; 47: 113-117.
[33] Ohshima H, Tatemichi M and Sawa T. Chemical basis of inflammation-induced carcinogenesis. Arch Biochem Biophys 2003; 417: 3-11.